# Development of Control Contraction Metric based methods on non-conventional aircraft configuration

J. Alonso-Pardo<sup>1</sup>, Manuel Sánchez Rubio<sup>2</sup>, and Óscar Rodríguez Polo<sup>3</sup>

<sup>1</sup>Flight Mechanics Area at Sub-directorate of Aeronautic Systems, Instituto Nacional de Técnica Aeroespacial 'Esteban Terradas' (INTA), Torrejón de Ardoz, Spain

E-mail:, alonsopj@inta.es

<sup>2</sup>Computer Science Department, University of Alcalá de Henares (UAH), Alcalá de Henares, Spain

E-mail:, manuel.sanchez@uah.es

<sup>3</sup>Automatics Department, University of Alcalá de Henares (UAH), Alcalá de Henares, Spain

E-mail:, o.rodriguez@uah.es

## **Abstract**

Control Contraction Metrics (CCMs) can be described as a non-linear control technique based in differential dynamics on the framework of differential geometry. This work presents preliminary results on applying CCMs to the control of a Blended Wing Body (BWB) aircraft configuration, in particular, regarding flight conditions involving high angle of attack and medium Reynolds number regimes. These preliminary results show that in absence of conventional stability equilibrium points, proper CCMs may allow effective control on aircraft dynamics given adequate operational conditions. These conditions and configuration are expected to be present in new concepts of Remotely Piloted Aircraft Systems (RPAS), extending their applications from planetary exploration to support the development of new transportation concepts in commercial airliners. Methods described, data, and results, are expected to be of application for Experimental Aircraft for European Leadership in Aviation (EXAELIA) project, a Horizon Europe international effort to de-risk and develop new concepts of passenger aircraft to face aerospace industry challenges by 2050.

This work has been funded by the European Union under GA No. 101191922. Views and opinions expressed are however those of the author only and do not necessarily reflect those of the European Union or the European Climate, Infrastructure and Environment Executive Agency. Neither the European Union nor the granting authority can be held responsible for them.

**Keywords:** Control Contraction Metrics Remotely Piloted Aircraft Systems Blended Wing Body EXAELIA Non-Linear Control

## 1 Introduction

## 1.1 CCMs in aerospace

Contraction can be roughly described as a dynamic system property capable of ensuring that under given circumstances, a trajectory in the system's state space contracts to another trajectory [1]. CCMs are sometimes presented as a non-linear control technique able to take advantage of this contraction property. By finding a suitable matrix metric in the manifold that contains the dynamic system, as long as the right conditions are accomplished by the metric and the system, theory

is able to predict if trajectories contraction is possible. Up to some extent, contraction shares characteristics with Lyapunov theory, and because of that, some authors present CCMs as a generalization of Lyapunov control techniques [2], or even a generalization of Lyapunov results, using as base for the claim the *Linear Matrix Inequalities* (LMI) sometimes used to calculate the metric matrix [3]. While Lyapunov functions are a very studied and developed topic in RPAS for both observers, such as [4], and controllers, for instance [5], CCMs seem like not so broadly applied in aerospace, maybe due the novelty of the research field, or due the numerical nuances

present in the development of practical solutions so far. Said nuances are mainly related to both obtaining the metric and its geodesics in order to develop feasible control laws.

These control laws can be developed and used both in open [6] and closed loop [7], including adaptations to adaptive control loops [8] accepting in this manner some levels of model uncertainty in the control. There also exist generalizations on the very same established theory on CCMs, extending the metrics on the manifold used (typically Riemann-like), to Finsler manifolds [3] [7], providing a more general framework in which develop both loop controllers and analysis.

As already mentioned, while Lyapunov techniques are widely applied in aerospace, CCMs may have not been extensively applied to aircraft control up to date, mainly due to the challenges of computing what is needed to achieve control in real time. The most interesting experimental work is maybe [9], in which authors deal with quadrotor trajectory tracking and obstacle avoidance by finding the metric needed offline, while the control is generated online, achieving fast and responsive maneuvers in indoor tests. Another remarkable result can be found on [10], where an attitude tracking controller for a fixed wing model is developed in simulation and used on equilibrium points of the linearized flight mechanics equations. Also in the realm of simulations, diverse remarkable results can be found related to CCMs theory development, for instance, in the context of trajectory tracking in robotics combining CCMs with machine learning [11], aerospace Control Contraction Metric (CCM) applications strongly based on optimization [12], or even combining both optimization and learning [13]. In [12] a robust controller for a powered descent module is obtained based on fuel optimization. In [13] a CCM is used to provide a fast way of learning and using control changes in a F-16 aircraft model, implementing also a CCM based controller.

So far we have not found works that tackle the direct control of non-linear equations for a non conventional configuration such as a BWB aircraft, using CCMs, relying on fast numerical methods beyond, for instance, optimization or *Sum of Squares* (SOS) programming. The contribution presented here is not intended to expand CCMs theory, but to be applied in the most practical manner, predicting contraction characteristics for a very preliminary non-conventional aircraft configuration. We also try to justify with simulated results on preliminary models that the contraction appears in an attitude tracker, allowing effective non-linear control in flight conditions that are difficult to manage otherwise, or at least by means of linear controllers.

The motivation for performing such work in a nonconventional aircraft configuration relies in the need of looking for new features and capabilities in RPAS both in Earth and space applications.

## 1.2 New features mean new control needs

Non-conventional aircraft configurations aim to offer new functionalities and desirable performance characteristics in aerospace applications. In the case of BWB configurations, drag reduction and therefore power consumption savings is maybe the most atractive of said features. In the field of plan-



Figure 1: Left: NASA's Ingenuity [14] is up to date the only RPAS able to fly atmospheric missions on another planet. Right: Different configurations have been proposed as planetary exploration RPAS, for instance, Prandtl-m concept [15]

etary exploration this is of remarkable importance, since size constraints and energy consumption reduction may determine the mission capabilities of a RPAS [16]. So far, the unique case of Ingenuity flights in Mars [14], justified a coaxial rotor solution, while other projected autonomous vehicles opted for conventional but especially also non-conventional configurations such as BWB-like designs [17]. Since constraints and decisions on design are determined by the mission, Earth and out-of-Earth applications can justify very different designs. In any case, looking for alternatives where these applications share difficulties can certainly benefit both.

Reduction in energy consumption is a common goal both in space exploration and airborne transport here at Earth. It is a constant and yearned goal in passenger aircraft, specially in the European scenario in which European Commision impulses initiatives [18] to achieve efficency in future transport aircraft. One of these initiatives is EXAELIA, an European effort to de-risk uncertainties for aircraft future technologies [19]. This work and its results are expected to be of application in said project, EXAELIA, as a part of one of the INTA's contributions this international collaboration.



Figure 2: INTA's three contributions to EXAELIA. The selection of a suitable flight test site for project next phases (left) comes with the use of Sistema Portable Óptico de Trayectogaría or Optical Portable Trajectography System (SPOT) (center) for on-ground measurements of flight testing demonstrators flights. Hazardous Flight Conditions (HFCs) control laws for said demonstrators is the third leg of INTA's contribution. Up today, several mock-ups have been printed at INTA (right) to identify main stability issues on BWB configurations. Final EXAELIA configuration is yet to be defined as a team effort between several international partners.

Achieving drag reduction is a very attractive goal but it comes with unavoidable trade-offs. While BWB configuration can offer remarkable drag reduction figures [20], it also brings on the table new difficulties in control related both to static

and dynamic stability [21]. Lateral-directional control is one of the main challenges, since a BWB will have low drag if vertical stabilizers are not present during flight. While flying without vertical stabilizers is certainly possible, as for instance *B-2 Spirit* aircraft proves, it also certainly complicates control beyond the safe-proven, traditional solutions present in conventional configurations such as the *Tube and Wing* (TAW), specially if we are in the domain of civilian passenger transport. In the domain of space exploration, on the other hand, where passengers are not expected to be on-board, achieving a completely safe, autonomous, and deterministic control is paramount for the success of the mission. Where a remote pilot can't act in time due to delays in communication, having a reliable and flexible control is undeniable of the outmost importance.

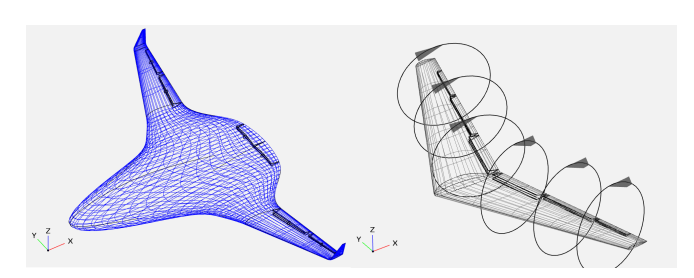


Figure 3: OpenVSP has been used to test preliminary solutions for non-conventional configurations. Kruger's (up left) BWB freely available at [22] has been modified by Rodrigo López at INTA to obtain aerodynamic information about a typical BWB configuration. A flying wing based in the Northrop N-9M design (up right) was also used to obtain know-how on drag rudders and non-conventional aerodynamic data. These modifications were possible to the work of Amalia Mucea, at Flight Mechanics Area at INTA.

Dynamics, uncertainties and the novelty of the application invite to looking for new ways of problem solving. In the case of BWB configurations regarding control, the way proposed in this work is tackling the non-linear dynamics of the system with minimal linearizations, in a manner that ensure, up to the system capabilities, that an actual control is possible. In order to do so, CCMs is proposed as tool.

### 2 CCMs

### 2.1 CCMs as a control technique

The explanation that follows in this section is a summary and interpretation of results extracted mainly from [2] and [6]. It is introduced here to stablish context for the work done. We can have a dynamic system described by Equation 1.

$$\dot{x} = f(x, u) \tag{1}$$

The system defined in a n-dimensional real vector space can be embedded into a manifold, in which we can define a metric matrix M able to determine distances between elements. Due

to embeddedment, since elements can be considered as vectors of state-space variables, the distance between two close elements can be defined as:

$$d = \delta_x M \delta_x' \tag{2}$$

Where  $\delta_x$  is the difference between these two close elements. At the same time, by constraining system (1) to an affine-control equation, it can be written as:

$$\dot{x} = f(x, t) + Bu \tag{3}$$

Where in Equation (3) B is a matrix that links u, the control vector, with the vector of state variables x. Now, if [6]:

$$-\frac{\partial M}{\partial t} - \sum_{i} \frac{\partial M}{\partial x_{i}} \dot{x}_{i} + \sum_{j} \frac{\partial M}{\partial u_{j}} + AM + MA^{T} + 2\lambda M - \rho BB^{T} < 0$$
(4)

Being in Equation (4)...

$$A = \frac{\partial f}{\partial x_i} + \sum_j u_j \frac{\partial u_j}{\partial x_i} \tag{5}$$

Then we can say our system is contracting in the points of the manifold that hold (4). Known terms in these expressions are matrices A and B, while matrix M, term  $\lambda$ , and scalar function  $\rho$  have to be fixed or found. The result of this expression is a symmetric matrix and therefore, a check on negative definiteness can be made by ensuring the sign of its eigenvalues are all negative.

Meaning of Equation (4) is not as complicated as the equation itself: we only have to find a suitable metric that ensures distances between points decrease as time goes by. The cause for this reduction in distances, for this contraction, has to be only due to the system dynamics and not to other artifacts. We can be sure of that for all points of the manifold in which M is a positive definite matrix (as all good metrics should), and Equation (4) provides a negative definite result.

Once the metric has been found, the next step is to find the geodesics  $\gamma$  this metric generates. These geodesics will have a strong connection with the control. They will provide the inputs u to make the initial trajectory to contract to the desired trajectory by applying the controls [23] [24] given by Equation (6):

$$u - u^* = -\int_0^1 \frac{1}{2} \rho B^T M \gamma_s(s) ds$$
 (6)

Where  $\rho$ , M, and B are known at this point, but shall be parametrized in the parameter s. The values  $\gamma_s$  are the first derivatives of the geodesics, also in s. u is the control we should apply, while  $u^*$  is the control already present in the system, which can be named as nominal control [23]. Of course, control in this context will be understood as open

loop control.

In summary control steers the system, control depends on geodesics, geodesics depend on metric. The proper metric will not only define the geodesics, but also can ensure that contraction exists (or at least the domain in which the contraction exists).

Being this work more focused in offering an application than discussing the theory, a lot of important details in notation and rigor has been left behind. One of uttermost importance is that these equations and results are only valid in manifold regions free from discontinuities and singularities (smooth). Another interesting matter is that notation is very influenced by the method developed for finding solutions. Looking for  $W = M^{-1}$  instead of M is a good example of this, since looking for W is one of the conditions needed to make convex the numerical search for the metric [6]. Another factor is that metric matrix has to be bounded and definite positive, and of course, in order for the controller to exist, the Equation (6) has to be path integrable.

### 2.2 Choosing CCMs

When the experts of the theory rely on numerical methods [6], [2], [25] for finding CCMs, looking for non numerical alternatives to do so is probably not a good idea. Searching for them can however help to understand the problem and the control proposed.

Equation (4) can be separated in:

$$-\frac{\partial M}{\partial t} - \sum_{i} \frac{\partial M}{\partial x_{i}} \dot{x}_{i} - \sum_{i} \frac{\partial M}{\partial u_{j}} + 2\lambda M < 0$$
 (7)

and

$$AM + MA^T - \rho BB^T \prec 0 \tag{8}$$

For Equation (8), a general solution can be found on [26]. Assuming  $M = M^T$ , and if we are careful with notation, we will have that it is possible to obtain a metric with Equation (9):

$$M = -\frac{1}{2} (A^T)^{\dagger} (-\rho B B^T) - U U^T A + V A + (I - (A^T)^{\dagger} A^T) Y$$
(9)

Where  $(A^T)^{\dagger}$  refers to the Moore-Penrose pseudinverse (a generalization of inverse matrix) of the matrix  $A^T$ . This formulation is tempting, since allows to directly compute a metric once the system is known; this is so with the added interest of the degrees of freedom of matrices U,V and Y, which despite having to comply with several conditions, are more or less arbitrary and can help to shape matrix M into a positive definite diagonal. Equation (7) can also be simplified as long as we assume a metric non dependent on inputs and time, but dependent on state space variables. If that is the case, since we can calculate the metric thanks to Equation (9), Equation (7) transforms into a serial of inequalities that can work as compatibility conditions in the state space

variables for the metric to contract.

This can yield results for very simple control systems, but unfortunately not in the case of this work. The reasons are Equation (9) does not guarantee a positive definite metric in general, and once the system is complicated enough, equations and expressions grow in difficulty. Suddenly, all the possible advantages of the application of analytical solutions vanish with the need of using numerical methods to solve non-linear algebraic equations that, in general, do not present guarantees of convergence.

We can extract interesting ideas from these expressions, though. And that will be helpful for Section 3. We can learn, for instance, that using a constant metric will not comply with Equation (7), since  $\lambda$  has to be a positive value. Therefore, for constant metrics we have to take into account only Equation (10):

$$AM + MA^T - \rho BB^T + 2\lambda M < 0 \tag{10}$$

Which clarifies an opposite relationship between  $\lambda$  and  $\rho$ . The parameter  $\lambda$  is often called rate of convergence and accounts for a superior limit in the convergence of the system. In order for our system to converge with a rate given by  $\lambda$ , the scalar function  $\rho$  has to increase to make negative definiteness possible. Rate of convergence system can be understood better graphically in Figure 4.

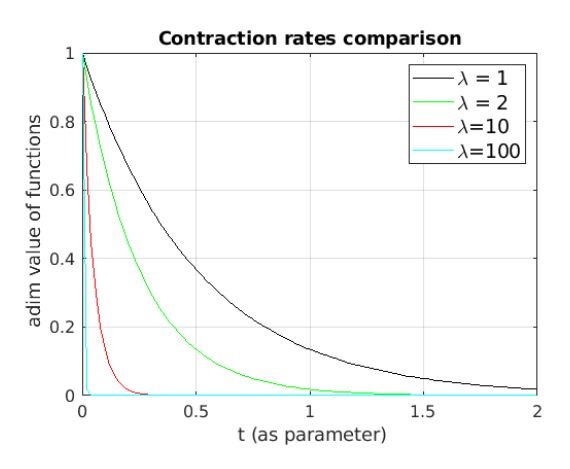


Figure 4: Comparison of contraction rates. Choosing a small value of  $\lambda$ , like  $\lambda=1$ , can make the system uncontrollable if response time has to be obtained under a certain time limit. A very high value of  $\lambda$ , such as  $\lambda=100$  may be physically infeasible if system can't react fast enough. It will depend on the system, of course, but for physical rotational systems, choosing  $20 > \lambda > 5$  seems reasonable as a first approach in contraction rate.

Using this meaning is of interest since it points out that a very high value of  $\lambda$ , although desirable to control the system faster, will only actually work in a system capable of such fast response. In general we won't be able to increase rate of

convergence as much as we want because contraction won't be possible, so not all contracting metrics will hold with all values of  $\lambda$ .

Another important factor that appears in Equations (7) to (10) is the scalar function  $\rho$ . It ensures the rate of contraction chosen can be achieved. We can assure this by choosing a higher value of  $\rho$  than  $\lambda$ , at least in simple systems. Also, since  $\rho$  is a scalar function, it can't be used to equilibrate the possible orders of magnitude differences in matrix B. Looking for this equilibrium is a good idea in our case, since we have preferred having all variables controllable in comparable response times due to its coupling. Due the nature of  $\rho$  this has to be done in the control expressions, though.

Choosing a baseline metric with all of the above considered, is straightforward: we can go with the identity matrix and see what happens to condition (4). We also can use the system described in Section 3, by Equations (15)-(17). They have as variables the typical angular rates p,q,r in body aircraft frame. In doing so, the system will describe a simplified rotational dynamics of a solid rigid.

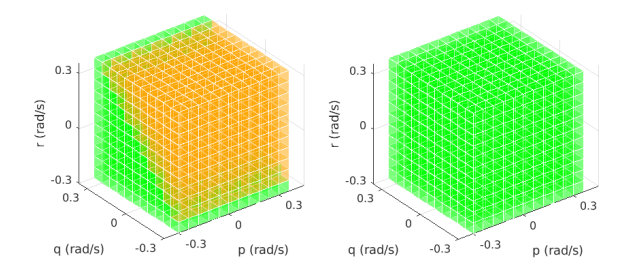


Figure 5: Discretization of domain in Equation (4) with identity metric. Orange means contraction is not guaranteed. To the left  $\rho=11.24\cdot 10^3$  with  $\lambda=10$ . To the right, the same  $\lambda$  with  $\rho=11.5\cdot 10^3$ .

Figure 5 is a 3D representation of state space variables domain (angular rates p,q,r), in between  $\pm 0.3$  rad/s. Each small cube inside the big one represents three values for p,q,r. The big cube represents the rough discretization of the domain of all possible variable values. The colors indicate if Equation (4) results in a negative definite matrix (green), mixed sign eigenvalues (orange), a completely positive definite matrix (red), or non-real eigenvalues (blue). Last two cases do not appear in this work. As expected, green is good: contraction is possible for these ranges of values. The other colors do not guarantee contraction, and therefore are zones we should avoid.

In the case of the identity matrix as metric, once we have fixed the desired  $\lambda$ , we should only change  $\rho$  to make the system contracting. That is, as long as our system allows the rate of contraction we have selected.

Trying other metrics will lead to different results. For instance, let's say we consider the metric:

$$M_{pqr} = \begin{bmatrix} p^2 & 0 & 0\\ 0 & q^2 & 0\\ 0 & 0 & r^2 \end{bmatrix} \tag{11}$$

A metric matrix that measures distances by applying penalties to them if angular rates are bigger than one. Clearly defined positive, we can check how it behaves in the same domain considered for identity metric.

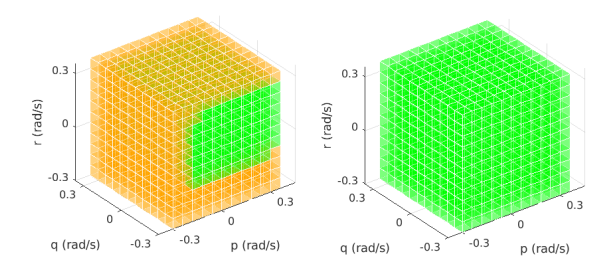


Figure 6: Discretization of domain for checking Equation (4) on metric  $M_{pqr}$ , Equation (11). Also for  $\lambda=10$ , to the left, the result of a poor contraction domain given by  $\rho=400$ . Due the derivative term,  $\rho=400$  can be smaller than in the identity metric case to ensure contraction. To the right, a complete contraction domain with  $\rho=1200$ 

Since it is not a constant matrix, the derivative term from Equation (7) is certainly helping. In this case  $\rho$  can be smaller, which could be interpreted that we can have contraction with less input control. This could serve our purposes if the control is suitable.

Finally we can try a metric that imposes a different penalty on values for p,q,r:

$$M_{exp} = \begin{bmatrix} e^{-2p} & 0 & 0\\ 0 & e^{-2q} & 0\\ 0 & 0 & e^{-2r} \end{bmatrix}$$
 (12)

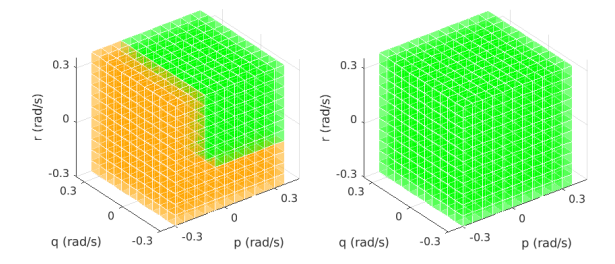


Figure 7: Discretization of domain for checking Equation (4) on metric  $M_{exp}$ , from Equation (12). Also for  $\lambda=10$ , to the left, the result of a poor contraction domain given by  $\rho=14\cdot 10^3$ . To the right, a complete contraction domain with  $\rho=21\cdot 10^3$ . It seems in this case the derivative term did not help to achieve negative definiteness.

The exponential metric achieves contraction in the domain of interest after incrementing  $\rho$ , above the  $\rho$  values used for the

quadratic metric. This means that in this case,  $M_{exp}$  may need more input effort than quadratic matrix, but in any case contraction seems possible.

By comparing these three discretizations, it also seems possible to use any of them to control the pure rotational system. Therefore, all of them shall be tested in section 4.1.

#### 2.3 Finding geodesics and calculating the controls

Finding geodesics can be a whole different problem on its own. Once the metric is known or chosen, a general analytical expression can be used to obtain the differential equations which solution is precisely the geodesics, in particular:

$$\frac{d^2x^a}{ds^2} + \frac{1}{2}g^{ad}\left(\frac{\partial g_{jd}}{\partial x^i} + \frac{\partial g_{id}}{\partial x^j} - \frac{\partial g_{ij}}{\partial x^d}\right)\frac{dx^i}{ds}\frac{dx^j}{ds} = 0 \quad (13)$$

Where x stands for the state variables of the system, s the parameter in which the geodesic is calculated on, and  $g_{ij}$  are the elements of the metric matrix.

The pursue of a diagonal matrix can be better understood by looking at Equation (13): crossed terms equal to zero will simplify the results deeply. A constant matrix also results in a very simplified expression that determine the geodesic as straight lines. For other metrics tested, the open source software MAXIMA has been used in order to obtain analytical expressions of the differential equations. Integration to obtain the geodesics from these differential equations has been done numerically with MATLAB software where analytical expressions were not easily obtained.

Regarding control through Equation (6), it has been implemented also in MATLAB by means of recalculating the integral in intervals of 0.1 s. Final results for control can be checked on Section 4. Before that and in order to continue, it is needed to finally present the dynamic system.

## 3 CCM on non-conventional aircraft configuration

The objective is to find a control based on CCMs able to take a BWB-like dynamic system safely from HFCs to a new flight condition in which a standard linear-control can regain authority. The reasons for this are:

- We can provide operating value ranges for the HFCs controller. That means, if we know when the HFCs controller can act, the nominal linear control will know when and how to depend on it. Sharing this information is critical to achieve a complete control coordination.
- Studying the controls needed to recover from HFCs can
  offer important information to the process of preliminary
  sizing for aircraft controls and systems. That is, since
  these preliminary calculations are going to tell us what
  are the torques needed to restore system dynamics, being
  sure our surface controls can deliver will tell us if we are
  in the right track.

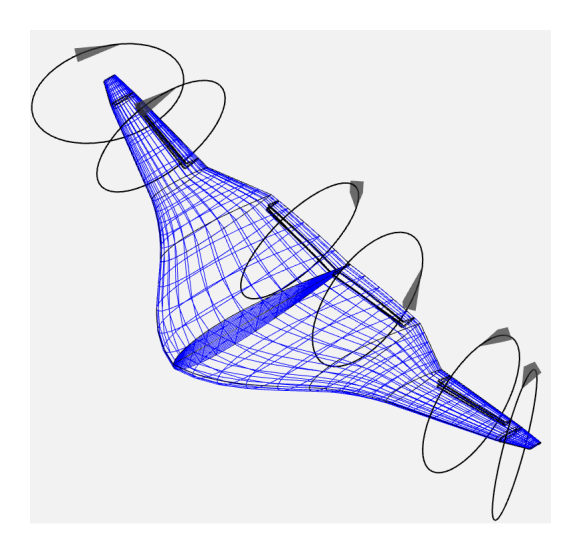


Figure 8: OpenVSP has also been used to model the preliminary BWB aircraft presented in this work. In absence of vertical rudders, whole wing-tip rotation will be used in a simplified model for rudder control. No engines, pods or other control surfaces than elevons and ailerons are present. This design will definitely change in the near future, but it is considered as representative of BWB main features.

By HFCs we are going to consider medium Reynolds number regimes and high angles of attitude. How small is small and how high is high can be open to interpretation so we are going to consider:

- Small Reynolds numbers may affect in both the reduction of control effectiveness [27] and in reduced control torques and forces due to small dynamic pressure. Our Reynolds regime near the stall region in Earth applications will be over Re = 300,000 which can be considered in the medium range, but will be modeled with a 10% reduction in control effectiveness anyway. For a mission in Mars the same flight conditions may appear around Re = 50,000, which would require a higher effectiveness reduction, as high as 40% in some cases [27].
- High angles of attack can produce stall, unexpected lateral forces and velocities, and also a reduction in control authority. We will use force and torque coefficients for a flight condition around  $\alpha = 10^{o}$ . For all the coefficients approximated with OpenVSP VLM solver, therefore we will be applying a effectiveness reduction of 10%.

These flight conditions can appear during different flight phases such as landing, take-off and spin induced stall. The objective of the control, as introduced earlier, will be to steer the system to a situation in which a standard linear control can operate safely the system (angular rates equal to zero or very close to zero).

## 3.1 BWB system and model characteristics

We will focus only in rotational dynamics. That is, our simplified system will only deal with reducing angular rates to zero

or close to zero in a reasonable period of time. Therefore, we can say:

$$\dot{w} = -w \times Jw + \frac{T}{I} \tag{14}$$

Where J is the inertia tensor, w and  $\dot{w}$  the angular rates and accelerations in typical airframe body axis p,q,r, being also T the torques. Equation has been programmed following formalism found in [28] which extends the equations as:

$$\Gamma \dot{p} = J_{xz}(J_x - J_y + J_z)pq - (J_z(J_z - J_y) + J_{xz}^2)qr + J_zl + J_{xz}n$$
(15)

$$J_{y}\dot{q} = (J_{z} - J_{x})rp - J_{xz}(p^{2} - r^{2}) + m$$
 (16)

$$\Gamma \dot{r} = -J_{xz}(J_x - J_y + J_z)qr + (J_x(J_x - J_y) + J_{xz}^2)pq + J_{xz}l + J_xn$$
(17)

With  $\Gamma = J_x J_z - J_{xz}^2$ , being l, m, n the torques in x, y, z body axis (roll, pitch and yaw). Finally, p, q, r are the angular rates that Equation (3.1), encapsulated in w.

Once presented the equations, we can plug some numbers into the model.

Table 1: BWB data used for simulations

Variable		Value	Unit
Mass	m	5.2	kg
Span	b	1	m
Reference surface	S	0.32	$m^2$
Reference chord	c	0.32	m
Aerod. ref. velocity (stall)	$V_{stall}$	10.2	m/s
Max Lift before stall	$C_L$	2.5	(-)
Inertia comp. in $X$ axis	$J_{\scriptscriptstyle X}$	$4.236 \cdot 10^{-2}$	kgm <sup>2</sup>
Inertia comp. in $Y$ axis	$J_{\mathrm{y}}$	$3.527 \cdot 10^{-3}$	kgm <sup>2</sup>
Inertia comp. in Z axis	$J_z$	$4.517 \cdot 10^{-2}$	kgm <sup>2</sup>
Inertia prod. in $X, Z$ axis	$J_{\scriptscriptstyle XZ}$	$6.993 \cdot 10^{-4}$	$kgm^2$

For the inertia tensor components a constant mass distribution has been considered in OpenVSP. Previous versions of this work offered different and greater values for all of the characteristics of the model. A smaller version of the aircraft has been finally chosen in order to ease the construction and testing of a future test bed.

### 4 Results and discussion

### 4.1 Comparing the metrics

We will be considering top angular rates of  $\pm 0.30$  rad/s, which are above  $15^o/s$ . For attitude rates, this is quite a lot, and would require a desirable control response in under a few seconds. It is arguable that such fast changes and movements can produce more aerodynamic interferences and extra difficulties in control. Furthermore, there will be already initial forces and torques in the aircraft that should add an extra in difficulty. This completeness in the model

will be tackled in future works. For the moment we are interested in comparing the control response of our three main metrics, in order to obtain preliminary know-how on control capabilities.

For our constant identity metric matrix (baseline), the evolution of rates is depicted in Figure 9, while torques applied can be seen in Figure 10.

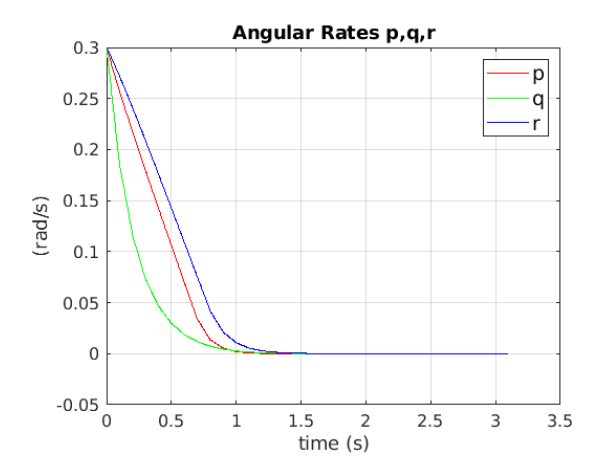


Figure 9: Angular rates evolution for the identity matrix as metric. Angular rates seem to reach stability under 2 seconds, which is a very desirable response.

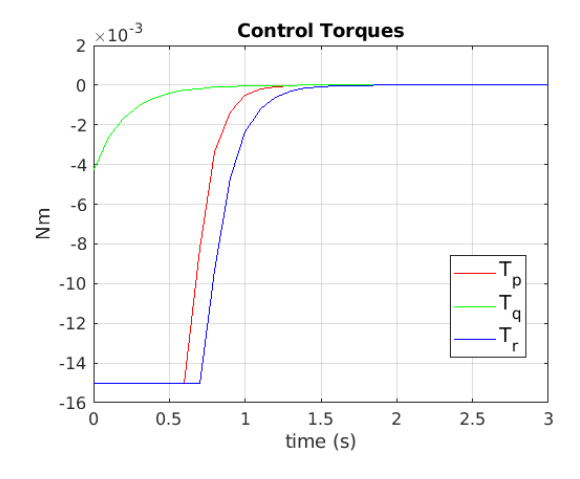


Figure 10: Control torques applied for the identity matrix as metric. A top torque of  $\pm 0.015$  Nm has been limited.

Identity matrix metric (and its control) gives an outstanding result. It provides a fast and strong response, controlling almost at the same time the three axis of rotation.

It may seem a good idea to simplify the control system by using the simplest of all metrics available, specially if we compare it with  $M_{pqr}$ , the metric with the squared angular rates from Equation (11).

If we study the torques provided by the control of  $M_{pqr}$ , in Figure 12, the reason for not controlling in time appears: torques are not sustained enough, which ends up slowing the response. This tendency is maintained over modification in  $\rho$ 

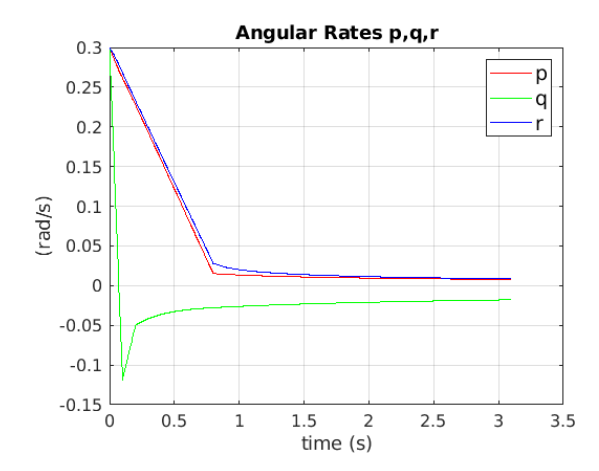


Figure 11: Angular rates evolution for the squared angular rates matrix metric  $M_{pqr}$ , Equation (11). Angular rates are controllable, but in an excessive quantity of time. While identity matrix could deliver in under 2 s, after almost 3 s, the  $M_{pqr}$  is unable to fully comply.

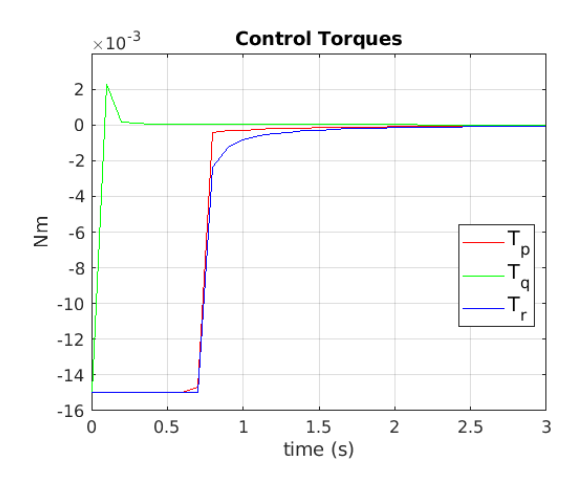


Figure 12: Control torques applied (down), for the squared angular rates matrix metric  $M_{pqr}$ , Equation (11). A top torque of  $\pm 0.015$  Nm has been limited.

values, so for the moment this metric has to be discarded for control.

Finally, we can have a look at Figure 13: the exponential metric  $M_{exp}$  response from Equation (12).

Response in Figure 13 and control torques in Figure 14 are very similar to the identity metric, so we could choose the identity constant matrix since integration of the geodesics in the exponential metric adds complexity.

There is also not too much difference between the two options when we deal with changes of sign in angular rates. It could be of interest not to steer the system to zero angular rates, but to actually looking for an opposed sign rate in order to return the attitude to normal. In this case, as Figures 15 and 16 show, identity metric is slightly slower in q and may need adjustments while  $M_{exp}$  seems just a little bit better. But in any case, this is not clearly determinant on which is better. More comparisons are needed to determine  $M_{exp}$  robustness. For future works a more detailed study in a more detailed system

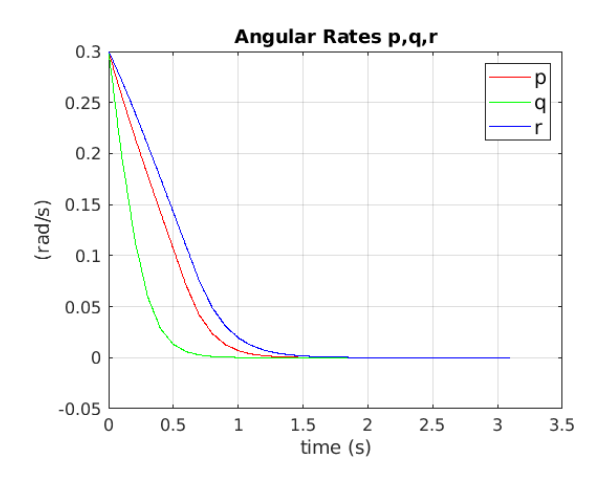


Figure 13: Angular rates evolution for the exponential angular rates matrix metric  $M_{exp}$ . Angular rates are controllable in a very similar way to identity metric based control.

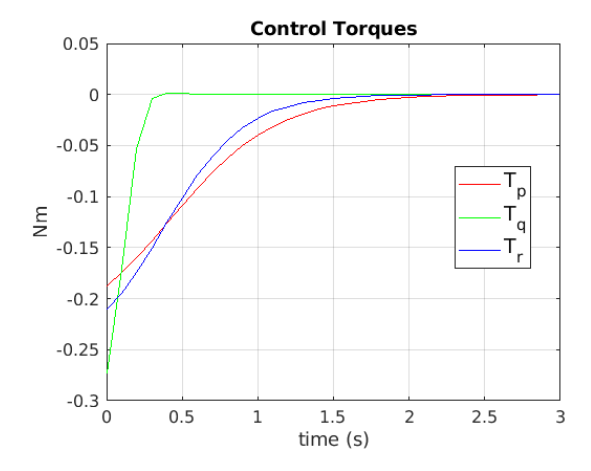


Figure 14: Control torques applied, for the exponential angular rates matrix metric  $M_{exp}$ . A top torque of  $\pm 0.015$  Nm has been limited.

may help to choose the best metric to be finally implemented.

## 4.2 A word on attitude control

So far we have compared the control response focusing only in getting the system to desired angular rates. In doing this simplified approach we have been able to compare different metrics, but we haven't tested a more representative problem which is steering the aircraft's attitude angles to desired (and safe) values.

This can be a problem on its own, since controlling the attitude is adding a complexity step to the simple rotational system tested so far. It can be made, however with a backstepping-like approach: we can select as simulation input the attitude angles, and by imposing a metric, obtaining through CCMs technique the desired rates. These desired rates can be controlled using as inner-loop the controller we have discussed and tested during the past sections.

A complete representativeness of the system, nevertheless, would require to add complete aerodynamic and engine forces and torques, initial conditions, and obtaining a complete tra-

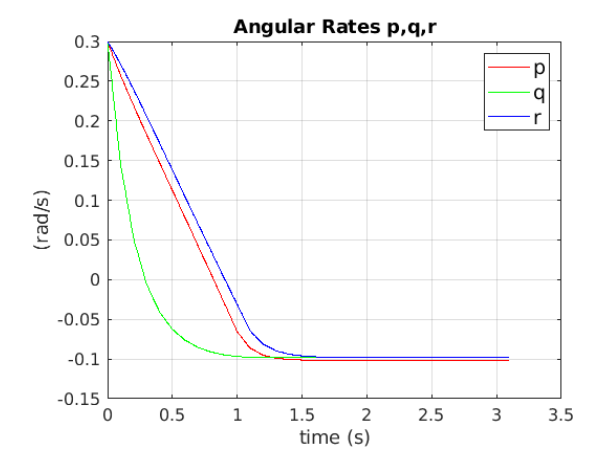


Figure 15: Angular rates evolution for the identity metric, with 0.3 rad/s as initial conditions to -0.1 rad/s as final commanded rates.

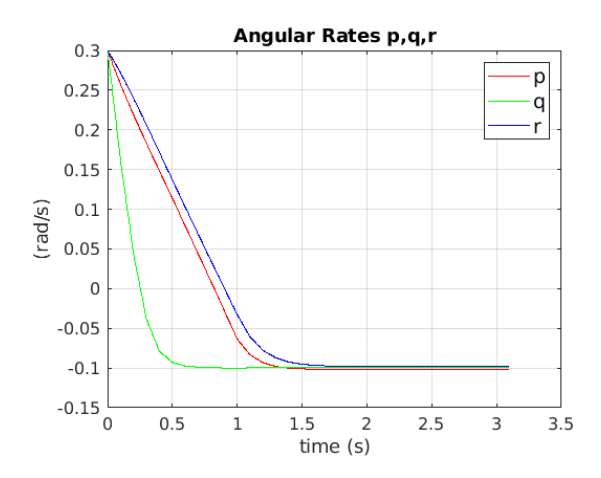


Figure 16: Angular rates evolution for the exponential metric, with 0.3 rad/s as initial conditions to -0.1 rad/s as commanded rates. Exponential metric matrix  $M_{exp}$  rates evolution slightly outperforms identity because is able to take the q closer to the final negative commanded value faster, but this difference is not considered determinant.

jectory evolution. However, in order to demonstrate the possibilities of the technique we have tested the identity and exponential metric with the attitude angle system defined by [28]:

$$\dot{\phi} = p + tan(\theta)(qsin(\phi) + rcos(\phi)) \tag{18}$$

$$\dot{\theta} = q\cos(\phi) - r\sin(\phi) \tag{19}$$

$$\dot{\psi} = (q\sin(\phi) + r\cos(\phi))/\cos(\theta) \tag{20}$$

Results are encouraging since with this simple approach it is possible to solve the backstepping problem with reasonable results, as can be seen of Figures 17 and 18. The only price to pay, is a small delay from one to two seconds in obtaining an acceptable attitude response. Reasonable control results are therefore obtained after 4 seconds. As it would be expected

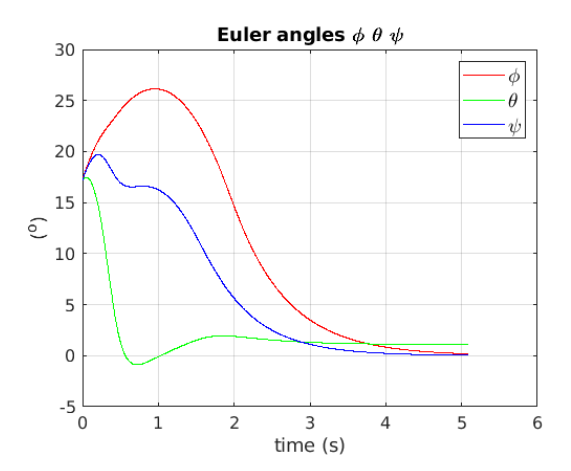


Figure 17: Attitude angles evolution, from a 0.3 rad/s initial condition both in rates and angles, to commanded zero attitude angles (and rates). A full zero is not reached with the identity metric in both systems, but results are good enough to ensure conventional control can regain authority.

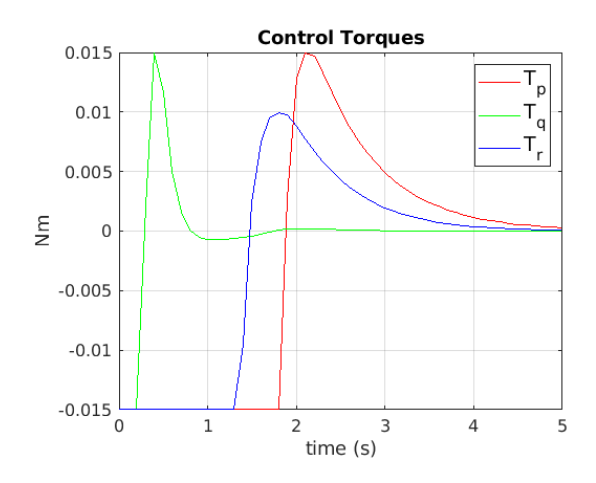


Figure 18: Control torques for the very same problem. In order to achieve zero, change on all torque signs are needed. Again, a saturation limit of  $\pm 0.015$  Nm is enforced.

by the results shown in Section 4.1, using the  $M_{exp}$  to the rate control, will improve a little bit the results by achieving closer to zero results in attitude angles. So, if instead using the identity metric as the metric for both rates and attitudes, we use for the rates  $M_{exp}$ , control is slightly better, as can be seen on Figure 19.

In summary, the baseline metric provides enough control authority for the system to return to a linear nominal control situation. Results can be slightly improved by using  $M_{exp}$  for rate control. For future works, we believe that modifying identity metric to a more real attitude dynamics model could improve the results presented.

## 4.3 Comparing the torques

Other point of interest is comparing the maximum torques and responses needed with the actual torques that representative control surfaces could provide. This comparison could offer some insight in what is going to be needed for a generic

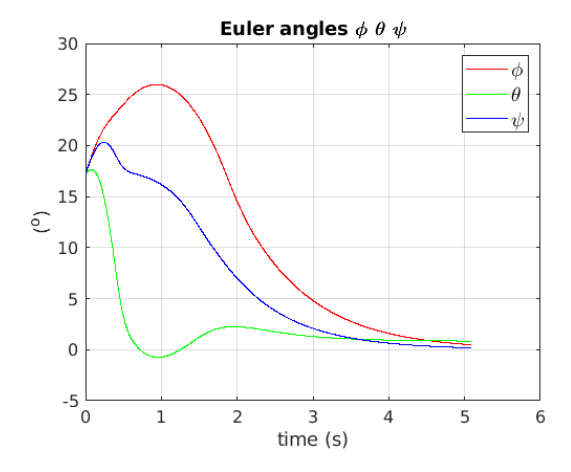


Figure 19: Attitude angles evolution, from a 0.3 rad/s initial condition both in rates and angles, to commanded zero attitude angles. For rate control,  $M_{exp}$  has been used. A full zero is not reached. Instead, all angles reach  $\pm 0.5^{\circ}$ .

BWB design. While not thorough, the analysis can be useful at least to ensure the torque limits imposed of  $\pm 0.015Nm$  are reasonable.

For pitch torque an actuation in the elevator will be used. For roll torque, ailerons will be applied. For yaw control, rotational capable wing tips will be considered. The reality may be more complicated than this simplification, since control allocation strategies shall be used to ensure actuator torques are consistent with torques needed, which is specially true if, as expected, activating a main control surface for one axis has dynamic coupling on others. Medium Reynolds and near to stall regime have been modeled by reducing available torques by a total of 20%. A summary of the figures considered can be found on Table 2. The influence of the aircraft base coefficient values is not considered in this comparison.

In Figure 20, aileron torques availability is shown.

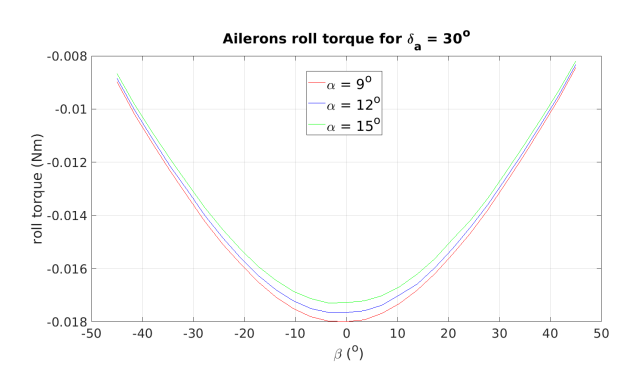


Figure 20: Roll torque available, for a maximum actuation of  $30^{\circ}$  in ailerons. The maximum roll torque applied of 0.015 Nm is achieved for a small range of  $\beta$  angles. Only control surface contribution to torque is displayed.

Roll torque is maybe the smaller of the controls available. This was not the case in initial iterations of this work, but it is for aircraft configuration presented in Figure 8. In any case is considered that up to  $\beta=\pm20^{\circ}$ , maximum torque can be achieved close to high attack angles. In Figure 21, pitch

torque contribution from the elevator is shown, again for three different attack angles.

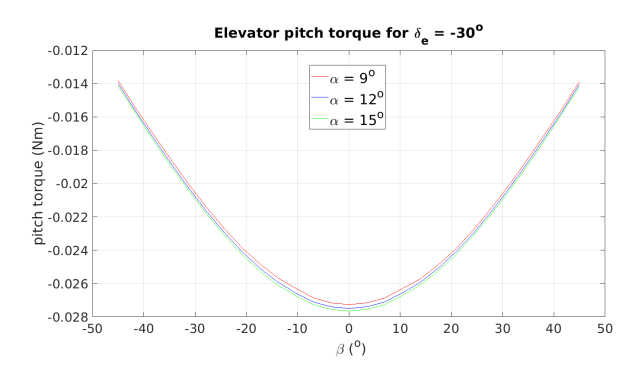


Figure 21: Pitch torque available, for a maximum actuation of  $-30^{\circ}$  in elevator. The maximum pitch torque applied of 0.015 Nm is achieved for a range of  $\beta$  angles of  $\beta = \pm 30^{\circ}$ . Only control surface contribution to torque is displayed.

Elevator contribution is a little bit higher and is present in an extended range of  $\beta$  angles. However the longitudinal control authority needed in both flying wings and BWB [21], recommend to have a greater elevator size and power to take aircraft base values into account. In future evolutions of this work, higher pitch control authority shall be obtained, specially to deal with situations in which aircraft base aerodynamic configuration does not help in achieving control.

Finally in Figure 22 yaw torque achieved by the wing tip rudder is considered.

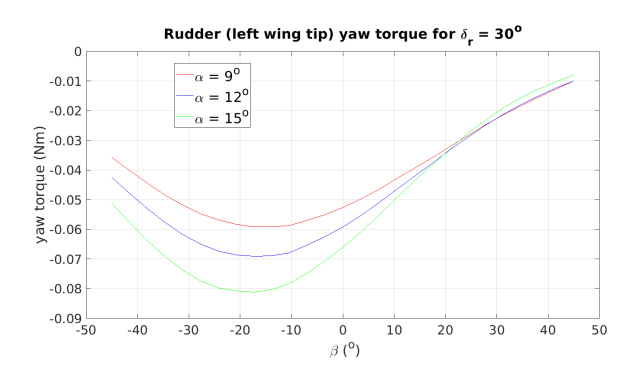


Figure 22: Yaw torque available, for a maximum actuation of  $30^{o}$  in wing tip rudder. The maximum yaw torque applied of 0.015 Nm is achieved for practically the whole range of angles  $\beta$  considered. Only control surface contribution is displayed.

In previous versions of this work, yaw control was the lowest of the torques available due the decision of using drag-rudders as directional controls. Typically in preliminary design for transport aircraft, vertical stabilizers can be sized by using the asymmetric power condition [29]. This tends to size tails with a surface maybe too great, but shows that a considerable stabilizer surface shall exist in order to gain lateral-directional control authority in all situations. This opposes a little bit the objective of offering low drag in BWB configurations and therefore, has to be treated carefully. Because of this, full rotational wing tip rudders have been considered in the BWB

configuration instead of vertical or drag rudders, achieving a high yaw control authority for practically the whole range of sideslip angles. The trade-off is the size and complexity of such actuators, altogether with the influence on other degrees of freedom beyond yaw, which shall be studied in detail in future works.

In summary what Figures 20, 21, and 22 point out is mainly the need for taking into account torque saturation in control strategies. It is also important to note that while design so far accounts for these maximum torques, aircraft base aerodynamic and engine torques, will certainly affect control authority making easier to regain control from some initial conditions and harder in others. For future works a more complete simulation is required to identify these situations, also accounting for actual flight conditions influence (such as  $\alpha$  and  $\beta$  angles) in control response. This preliminary work has served to correct the weak yaw control response and ensure a bare minimum torque authority is possible to achieve successful control with CCM control strategy.

Table 2: Maximum torques comparison in flight condition  $\alpha = 9^{\circ}$ ,  $\beta = 0$  and p, q, r < 0.3 rad/s

Variable		Value	Unit
Roll torque needed Available ( $\delta_a = -30^o$ )	$L_{max}$ $L$	$\pm 0.015$ up to $\pm 0.018$	Nm Nm
Pitch torque needed Available ( $\delta_e = -30^o$ )	M <sub>max</sub> M	$\pm 0.015$ 0.022 to $-0.027$	Nm Nm
Yaw torque needed Available ( $\delta_r = 30^\circ$ )	N <sub>max</sub> N	$\pm 0.015$ about $\pm 0.05$	Nm Nm

Another important matter is maybe the capability of the control surfaces in offering actual control in time. Time constants and actuator dynamics haven't been simulated in this simplified approach. While for small RPAS actuator response could be fast enough, this velocity in actuation shall be certainly taken into account in larger aircraft, as EXAELIA project certainly will demand.

### 5 Conclusions and future works

The development of CCM methods on non-conventional aircraft configurations was introduced. Firstly, an overview of the theory involved was described, followed by some practical insights regarding the election of a suitable CCM. After this, several remarks on a purely rotational system as model are also introduced. The main result in this part is maybe the importance of accounting for realistic system response and control, and their implication on the parameters involved in the CCM controller.

Several values for torques needed are also assessed providing a preliminary baseline for sizing actuators and control surfaces. This and other conclusions will be provided to EXAELIA project, as part of the HFCs control laws design task. Regarding future works it is imperative to check these results in the more general context of the complete Flight Dynamics of the aircraft, specially if a real physical model is tested in

real flight conditions or at least in controlled real conditions. Also, attitude control can be fully dealt with updating Equations (18), (19), and (20) to a quaternion approach, taking profit of the non-linear capability that CCMs use can provide, at least as long as control authority is provided. It would be also of interest to simulate complete critical maneuvers such as take-off, landing and spin induced stall, putting special care in the matter of absence of vertical stabilizers to recover from these flight conditions. The closed loop matter is yet to be addressed too, since the approach presented can be considered so far only a tracking solution. Following this line, it is also of interest to study the introduction of adaptive solutions and measures to deal with uncertainties both in the model and control.

## 6 Acknowledgements

Software used for this work includes MATLAB [30] for numerical simulations and calculations, and MAXIMA [31] for symbolic algebra matrix operations. Regarding MATLAB, Figures 5, 6, and 7, were obtained by modifying the code for 3D representation available at [32]. OpenVSP [33] was also used in this work to obtain inertia tensor information and very preliminary aerodynamic data. We would also like to acknowledge the work of Michael Kruger [22] offering online its desing under Creative Commons 0, and our intern Rodrigo López Azcoitia for his work modifying and working on Kruger's model at Flight Mechanics Area, at INTA. We also would like to thank our intern Amalia Mucea Mucea, whose work in the flying wing model has been of great value to gain insight in the Flight Mechanics Area on non-conventional aircraft configurations.

This work has been funded by the European Union under GA No. 101191922. Views and opinions expressed are however those of the author only and do not necessarily reflect those of the European Union or the European Climate, Infrastructure and Environment Executive Agency. Neither the European Union nor the granting authority can be held responsible for them.

### References

- [1] Winfried Lohmiller and Jean-Jacques E Slotine. On contraction analysis for non-linear systems. *Automatica*, 34(6):683–696, 1998.
- [2] Sigurdur Hafstein Peter Giesl and Christoph Kawan. Review on Contraction Analysis and Computation of Contraction Metrics. *Journal of Computational Dynamics*, 10(1):1–47, 2023.
- [3] Fulvio Forni and Rodolphe Sepulchre. A differential Lyapunov framework for contraction analysis. *IEEE transactions on automatic control*, 59(3):614–628, 2013.
- [4] Sergio de La Parra and Javier Angel. Low cost navigation system for UAV's. *Aerospace Science and Technology*, 9(6):504–516, 2005.

- [5] Thor I. Fossen Erlend M. Coates, Dirk Reinhardt. Reduced-Attitude Control of Fixed-Wing Unmanned Aerial Vehicles Using Geometric Methods on the Two-Sphere. 2020.
- [6] Ian R. Manchester and Jean-Jacques E. Slotine. Control Contraction Metrics: Convex and Intrinsic Criteria for Nonlinear Feedback Design. *IEEE transactions on automatic control*, 62(6), 2017.
- [7] Thomas L Chaffey and Ian R Manchester. Control Contraction Metrics on Finsler manifolds. In 2018 Annual American Control Conference (ACC), pages 3626–3633. IEEE, 2018.
- [8] Brett T. Lopez and Jean-Jacques E. Slotine. Adaptive Nonlinear Control With Contraction Metrics. *IEEE Control Systems Letters*, 5(1):205–210, 2021.
- [9] Anirudha Majumdar Jean-Jacques Slotine Sumeet Singh, Benoit Landry and Marco Pavone. Robust Feedback Motion Planning via Contraction Theory. 2019.
- [10] Yi Yu, Guo Zhang, Ping He, Heng Li, Jiannong Cao, and Feiqi Deng. Tracking attitude with sum-of-squares programming for a fixed-wing air vehicle. *IEEE Transactions on Circuits and Systems II: Express Briefs*, 69(8):3450–3454, 2022.
- [11] Dawei Sun, Susmit Jha, and Chuchu Fan. Learning certified control using contraction metric. In *Conference on Robot Learning*, pages 1519–1539. PMLR, 2021.
- [12] Brett T Lopez, Jean-Jacques E Slotine, and Jonathan P How. Robust powered descent with control contraction metrics. In 2018 IEEE Conference on Decision and Control (CDC), pages 3483–3490. IEEE, 2018.
- [13] Matthew Osborne. Safe online learning for nonlinear dynamical systems using control contraction metrics. PhD thesis, Cranfield University, 2023.
- [14] Haavard F Grip, Daniel P Scharf, Carlos Malpica, Wayne Johnson, Milan Mandic, Gurkirpal Singh, and Larry A Young. Guidance and control for a Mars helicopter. In 2018 AIAA Guidance, Navigation, and Control Conference, page 1849, 2018.
- [15] Nancy J. Pekar. Could this be the first Mars Airplane? https://www.nasa.gov/aeronautics/could-this-become-the-first-mars-airplane/, note = [Online; Accessed 1st June 2025].
- [16] Enrico Giacomini, Lars-Gran Westerberg, and George Nikolakopoulos. A Survey on Drones for Planetary Exploration: Evolution and Challenges. In 2022 30th Mediterranean Conference on Control and Automation (MED), pages 583–590. IEEE, 2022.
- [17] Mostafa Hassanalian, D Rice, and A Abdelkefi. Evolution of space drones for planetary exploration: A review. *Progress in Aerospace Sciences*, 97:61–105, 2018.

- [18] Clean Aviation Joint Undertaking. Clean Aviation. https://www.clean-aviation.eu/, note = [Online; Accessed 1st June 2025], 2025.
- [19] EXAELIA Consortium. EU-Project EXAELIA: Towards flying testbeds for novel long-range aircraft. https://exaelia.eu/, note = [Online; Accessed 1st June 2025], 2025.
- [20] Shanling Yang, Mark Page, and Ed J Smetak. Achievement of nasa new aviation horizons n+ 2 goals with a blended-wing-body x-plane designed for the regional jet and single-aisle jet markets. In 2018 AIAA Aerospace Sciences Meeting, page 0521, 2018.
- [21] Helena V de Castro. Flying and handling qualities of a fly-by-wire bwb civil transport aircraft. 2003.
- [22] Michael Kruger. Blended Wing Body on OpenAirshow. https://airshow.openvsp.org/vsp/uGjWQekFe6IobbfZrym0, 2025. [Online; accessed 2025-06-01].
- [23] Karen Leung and Ian R Manchester. Nonlinear stabilization via control contraction metrics: A pseudospectral approach for computing geodesics. In *2017 American Control Conference (ACC)*, pages 1284–1289. IEEE, 2017.
- [24] Dongjun Wu, Bowen Yi, and Ian R Manchester. Control contraction metrics on Lie groups. *arXiv preprint* arXiv:2403.15264, 2024.
- [25] Lai Wei, Ryan Mccloy, and Jie Bao. Control Contraction Metric synthesis for discrete-time nonlinear systems. *IFAC-PapersOnLine*, 54(3):661–666, 2021.
- [26] Yongge Tian. How to solve three fundamental linear matrix inequalities in the Löwner partial ordering. *Journal of Mathematical Inequalities* 8, 1–54, 2014.
- [27] Masayuki Anyoji, Masato Okamoto, Hidenori Hidaka, Katsutoshi Kondo, Akira Oyama, Hiroki Nagai, and Kozo Fujii. Control surface effectiveness of low Reynolds number flight vehicles. *Journal of Fluid Science and Technology*, 9(5):JFST0072–JFST0072, 2014.
- [28] Brian L Stevens, Frank L Lewis, and Eric N Johnson. Aircraft control and simulation: dynamics, controls design, and autonomous systems. John Wiley & Sons, 2015.
- [29] Egbert Torenbeek. Synthesis of subsonic airplane design: an introduction to the preliminary design of subsonic general aviation and transport aircraft, with emphasis on layout, aerodynamic design, propulsion and performance. Springer Science & Business Media.
- [30] MATLAB. Matlab v2012, 2025.
- [31] Maxima. Maxima, a computer algebra system. version 5.47.0, 2023.

- [32] Korosh Agha Mohammad Ghasemi. How can I plot a 3D matrix as a cube with different transparent colors for the values?, 2025. [Online; accessed 1st April 2025].
- [33] Rob McDonald J.R. Gloudemans et al. Open Vehicle Sketch Pad, 2025.